Weierstraß-Institut
für Angewandte Analysis und Stochastik

im Forschungsverbund Berlin e.V.

Preprint ISSN 0946 – 8633

Control and removing of modulational instabilities in low dispersion photonic crystal fiber cavities

Mustapha Tlidi [1], Arnaud Mussot [2], Eric Louvergneaux [2], Gregory Kozyreff[1], Andrei Vladimirov [3], Abdelmajid Taki [2]

submitted: 17th January 2007

[1] Optique Nonlinéaire Théorique,
Université Libre de Bruxelles,
C.P. 231, Campus Plaine,
B-1050 Bruxelles,
Belgium
E-mail: mtlidi@ulb.ac.be
Gregory.Kozyreff@icfo.es

[2] Laboratoire de Physique des Lasers,
Atomes et Molécules, UMR-CNRS 8523 IRCICA,
Centre d'Etudes et de Recherches
Lasers et Applications (CERLA) FR CNRS 2416,
Université des Sciences et Technologies de Lille,
F - 59655 Villeneuve d'Ascq, France
E-mail:Arnaud.Mussot@phlam.univ-lille1.fr
eric.louvergneaux@univ-lille1.fr
Abdelmajid.Taki@phlam.univ-lille1.fr

[3] Weierstrass Institute for Applied Analysis and Stochastics,
Mohrenstrasse 39, D - 10117 Berlin, Germany
E-Mail: vladimir@wias-berlin.de

No. 1201
Berlin 2007

WIAS

2000 *Mathematics Subject Classification.* 78A60,37K45.

Key words and phrases. photonic crystal fibers, modulational instability, forth order dispersion.

1999 *Physics and Astronomy Classification Scheme.* 42.65.-k, 42.65.Wi, 42.65.Sf.

Edited by
Weierstraß-Institut für Angewandte Analysis und Stochastik (WIAS)
Mohrenstraße 39
10117 Berlin
Germany

Fax: + 49 30 2044975
E-Mail: preprint@wias-berlin.de
World Wide Web: http://www.wias-berlin.de/

Abstract

Taking up to fourth order dispersion effects into account, we show that fiber resonators become stable for large intensity regime. The range of pump intensities leading to modulational instability becomes finite and controllable. Moreover, by computing analytically the thresholds and frequencies of these instabilities, we demonstrate the existence of a new unstable frequency at the primary threshold. This frequency exists for arbitrary small but nonzero fourth order dispersion coefficient. Numerical simulations for a low and flattened dispersion photonic crystal fiber resonator confirm analytical predictions and opens the way to experimental implementation.

Instabilities in non-equilibrium systems are drawing considerable attention both from fundamental as well as from applied point of views [1, 2]. One such instability gives rise to periodic self-modulations and is referred to as Modulational Instability (MI) in temporally dispersive media [3] and Turing instability [4] in spatially extended systems. In optical fibers, MI results from the interplay between chromatic dispersion and the intensity-dependent refractive index. In the usual scalar free propagation, the phase matching of the underlying four-wave mixing process requires anomalous dispersion [3]. However, phase matching can also be achieved in normal dispersion region by considering extra degrees of freedom such as polarization in birefringent [5] and isotropic [6] fibers, bi-modal fibers [7], working around the Zero Dispersion Wavelength (ZDW) [8, 9, 10] or inserting the fiber within a cavity [11]. Scalar MI in free propagation through a single mode optical fiber is usually described by the Non Linear Schrödinger Equation (NLSE) in which the propagation constant is expanded in a Taylor series in the frequency domain. It has been shown that only even order terms contribute to the MI gain and that development up to the fourth order must be considered when the pump wavelength is closed to the ZDW. In this case, scalar MI is possible in normal dispersion region if the fourth order dispersion term is negative and a second frequency of instability can be generated if the fourth order dispersion term is positive [8, 9, 10]. To our knowledge, intra-cavity MI leading to a single frequency has only been studied in relatively strong dispersion regions where models including up to the second order dispersion term are relevant to describe its dynamics.

In this letter, we show that it is necessary to take into account up to the fourth order dispersion term to capture the full MI dynamics of a passive fiber resonator, especially when proceeding close to the ZDW. To this end, we extend the model developed by Lugiato-Lefever [12] (LL model) up to the fourth order dispersion term. We then demonstrate that, however small the fourth order dispersion coefficient

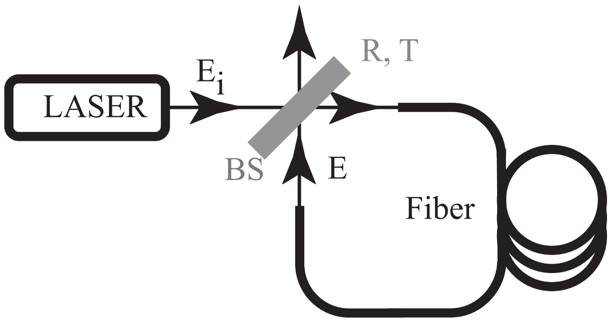

Figure 1: Experimental setup. BS : Beam Splitter.

is, a second frequency of instability can be observed at the primary threshold of stationary state destabilization which adds to the single one predicted and observed up to now [11]. Moreover, we demonstrate that the MI process has a finite domain of existence delimited by two pump power values, allowing for the stationary state to restabilize at large powers. We investigate the evolution of the MI frequencies within the existence domain from their rise up to their disappearance. Finally, in view of an experimental implementation, we perform numerical simulations for a realistic experimental configuration with a flattened dispersion photonic crystal fiber and find excellent agreement with the analytical predictions.

The fiber resonator is schematically depicted in Fig. 1. A continuous wave of power E_i^2 is launched into the cavity by means of a beam splitter, propagates inside the fiber and experiences dispersion and Kerr effect. At each round trip the light inside the fiber is coherently superimposed with the input beam. This can be described by the following boundary conditions $E(z=0,\tau+t_R)=T\times E_{in}(\tau)+R\times E(L,\tau)exp(-i\Phi_0)$ and by the following extended NLSE $\partial_z E(z,\tau) = (-i\frac{\beta_2}{2}\partial_{\tau^2}+\frac{\beta_3}{6}\partial_{\tau^3}+i\frac{\beta_4}{24}\partial_{\tau^4}+i\gamma|E|^2)E$, with t_R the round-trip time, Φ_0 the linear phase shift, T^2 (R^2) the intensity mirror transmissivity (reflectivity) and L the cavity length. The electric field inside the cavity is denoted E. $\beta_{2,3,4}$ are the second, third and fourth order dispersion terms respectively. γ is the nonlinear coefficient, z the longitudinal coordinate and τ the time in a reference frame moving at the group velocity of the light. This infinite-dimensional map can be simplified to the following single normalized equation by applying the mean field approximation:

$$\begin{aligned}\frac{\partial\psi}{\partial t'} &= S-(1+i\Delta)\psi+i\left|\psi\right|^2\psi-i\beta_2\frac{\partial^2\psi}{\partial\tau'^2}\\ &\quad +B_3\frac{\partial^3\psi}{\partial\tau'^3}+iB_4\frac{\partial^4\psi}{\partial\tau'^4} \qquad (1)\end{aligned}$$

where $t'=tT^2/2t_R$, $\tau'=\tau\left(T^2/L\right)^{1/2}$, $\psi=E\sqrt{2\gamma L/T^2}$, $S=2/T\left(2\gamma L/T^2\right)^{1/2}E_i$ the normalized input field, $B_3=\beta_3 T/\sqrt{9L}$, $B_4=\beta_4 T^2/12L$, and $\Delta=2\Phi_0/T^2$ is the cavity detuning. We carry out the analytical study in a low dispersive fiber

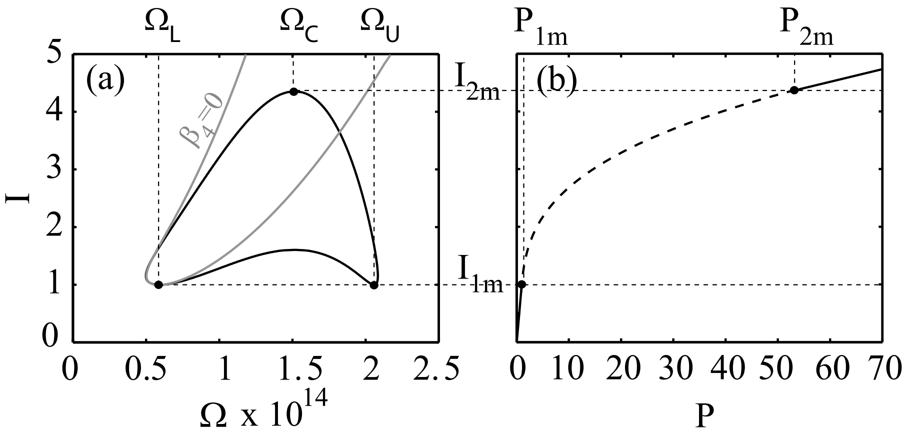

Figure 2: (a) Marginal stability curve for the steady state solution against MI. Black curve for $\beta_4 \neq 0$ and grey one for $\beta_4 = 0$.(b) Evolution of the cavity intensity stationary state $I = |\psi_S|^2$ versus the input intensity $P = |S|^2$ (the dashed line corresponds to the unstable case). $\gamma = 10\,W^{-1}.km^{-1}$, $\Phi_0 = 1.98\pi$, $T = 0.35$, $L = 10\,m$, $\beta_2 = -3 \times 10^{-28} s^2/m, \beta_3 = 0\; and\, \beta_4 = 6.4 \times 10^{-54} s^4/m$.

with a small dispersion slope. Thus, B_3 can be neglected. The steady state (SS) response ψ_S of Eq. (1) satisfies $S_S = [1 + i(\Delta - |\psi_S|^2)]\psi_S$. This solution is identical to the one of the LL model leading to a monostable (bistable) regime for $\Delta < \sqrt{3}$ ($> \sqrt{3}$). Its stability with respect to finite frequency perturbations, i.e. of the form $\exp(i\Omega\tau' + \lambda t')$ shows that the MI frequencies that can be destabilized at the primary threshold $I_{1m} = |\psi_{1m}|^2 = 1$ are

$$\Omega^2_{L,U} = \frac{-\beta_2 \pm \sqrt{\beta_2^2 + 4(\Delta - 2)B_4}}{2B_4}, \tag{2}$$

and it is immediate to see that two frequencies can be destabilized at the primary threshold for suitable choice of β_2 and Δ. Thus, taking into account β expansion up to the fourth order in Eq. (1) evidences the existence of a second frequency of instability, which had not yet been reported experimentally nor theoretically when working in quite strong dispersion regions [11].

This is illustrated by the closed marginal stability curve in Fig. 2(a), where two destabilization frequencies (Ω_L and Ω_U) exist at the primary threshold I_{1m} in the monostable regime [Fig. 2(b)]. The finite extent of the MI domain is also evidenced by the lower and upper values of cavity power $|\psi_{1m}|^2 = I_{1m} = 1$ and $|\psi_{2m}|^2 = I_{2m} = (2\Delta_{eff} + \sqrt{\Delta^2_{eff} - 3})/3$. The lower value fixes the minimum input power required for the MI process to occur, while the upper one can be tuned as a function of the physical parameter $\Delta_{eff} = \beta_2^2/(4B_4) + \Delta$. The critical value of the frequency at the upper bifurcation point I_{2m} is given by $\Omega_c^2 = -\beta_2/2B_4$ and we note that it satisfies the averaging relation $\Omega_c^2 = \Omega_L^2 + \Omega_U^2$. This result strongly contrasts with the usual cavity modulational instability where the instability domain is not bounded as shown on Fig. 2(a) by the gray lines. So the two main results of this stability analysis are (i) two instabilities at frequencies Ω_U and Ω_L occur simultaneously at the primary threshold (I_{1m}) and (ii) it is possible to restabilize or recover the stationary state by driving the system to the large intensity regime ($I > I_{2m}$).

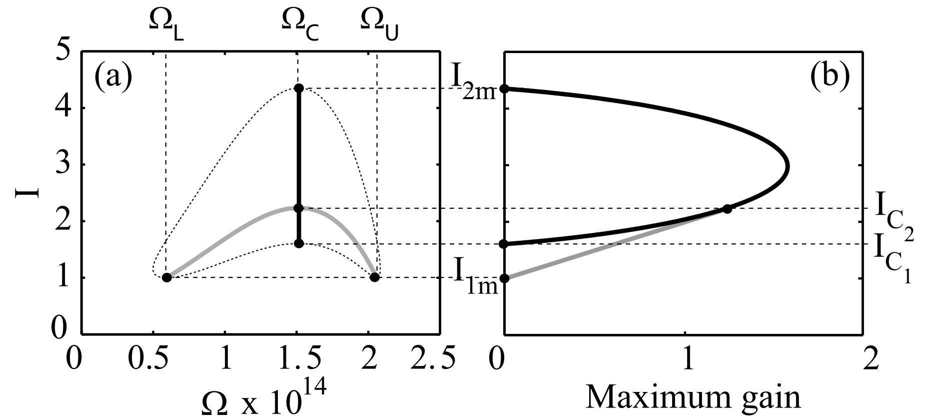

Figure 3: Evolution of the maximum temporal gains (black and grey continuous lines) versus (a) the frequency Ω and (b) the output intensity I.

In view of the above analysis, an important question arises: how do the first two frequencies Ω_L and Ω_U evolve and connect to Ω_c upon increasing the input intensity $P = |S|^2$? The linear stability analysis can give us some insight on this point through the evolution of the most unstable frequencies of the SS, as shown in Fig. 3. at $I \geq 1$ the SS undergoes a bifurcation leading to small-amplitude modulations at frequencies Ω_L and Ω_U. The two corresponding bands of unstable frequencies widens with growing I, until it reaches the value I_{c1} at $\Omega = \Omega_c$ [Fig. 3(a)]. This signals the merging of the two bands into a single, larger one. This new band of unstable frequencies is now characterized by the existence of three frequencies with positive gain, as can be seen from Fig. 4(b). When further increasing I, the two most unstable lateral frequencies merge into the critical one Ω_c at $I = I_{c2}$. This point indicates an outstanding feature leading to an exchange of the maximum gain between Ω_L (Ω_U) and Ω_c [Fig. 3(b)]. Finally, one then can expect from Fig. 3 that above this power value ($I > I_{c2}$), the dynamics is dominated by the frequency Ω_c until the upper limit of the instability domain is reached ($I = I_{2m}$).

These results should be experimentally observable using a fiber whose dispersion curve is low and as flat as possible at the working wavelength ($\beta_3 \approx 0$). We numerically checked our predictions by integrating the extended NLSE with bounded conditions by using the split step Fourier method with an input continuous wave. We included realistic third and fourth dispersion order term values in our simulations (see caption of Fig. 2). Indeed, we did not take exactly $\beta_3 = 0$ but a very low value ($D_S = 0.001\, ps/nm^2/km$ i.e., $\beta_3 = 2.10^{-42} s^3/m$) [13] to match with realistic configuration. We have checked in all our simulations that the final state was reached ($\simeq\sim$400 round trips). We show on Fig. 4(a) that two frequencies (0.98

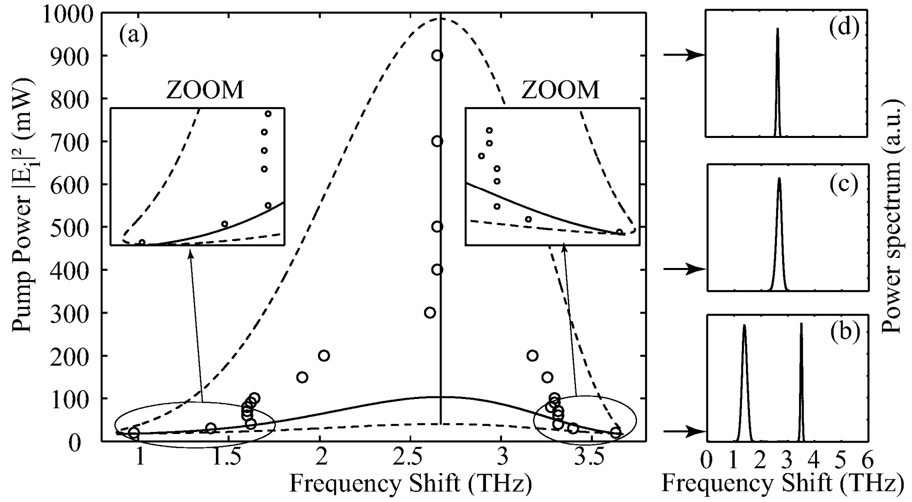

Figure 4: (a) Evolution of the frequency of instability versus the pump power with same parameters listed in Fig. 2 excepted for $\beta_3 = 2 \times 10^{-42} s^3/m$. Circles numerical simulations and full lines analytical results. (b), (c) and (d) power spectra for 30 mW, 400 mW and 900 mW of pump power respectively.

THz and 3.63 THz) are destabilized (circles) just above the first pump threshold (20 mW) [Fig. 4(b)] in excellent agreement with analytical results (1.1 THz and 3.6 THz). By increasing the pump power they merge together leading to a single frequency of instability arround 300 mW [Fig. 4(c)]. This unique frequency then disappears just above the second pump threshold corresponding to a recovering of the stationary state of the cavity. Thus, the two main predictions of our analytical study are numerically verified. This linear stability analysis provides an excellent insight of the frequency evolution scenario within the instability domain except for $50\,\mathrm{mW} < I < 300\,\mathrm{mW}$ [Fig. 4(a)]. In this last region only a nonlinear analysis as in [14, 15] will figure out the dynamical evolution of the system. This work is in progress.

To summarize, we presented an analytical and numerical study of a coherently driven photonic crystal fiber resonator. We showed that it is necessary to take into account dispersion up to the fourth order to capture the full temporal dynamics of the system. Namely, there exist two frequencies at the primary MI threshold, and their domain of existence is finite or bounded such that the stationary state is recovered for high enough intensity pumping. In addition, numerical simulations, carried out for realistic experimental parameters, provide the evolution of these instabilities with the input field. They confirmed our analytical results and constitute a step towards a future experimental demonstration.

M.T and G.K. received support from the Fonds National de la Recherche Scientifique (Belgium). This work was also partially supported by the Interuniversity Attraction Pole program of the Belgian government. The IRCICA and CERLA are supported in part by the “Conseil Régional Nord Pas de Calais” and the ”Fonds Européen de Développement Economique des Régions”.

References

[1] M.C. Cross, and P.C. Hohenberg, Rev. Mod. Phys. **65**, 851 (1993).

[2] G. P. Agrawal, Nonlinear Fiber Optics (San Diego, CA: Academic, 1995).

[3] K. Taï, A. Hasegawa and A. Tomita, Phys. Rev. Lett. **56**,135 (1986).

[4] A.M. Turing, Philos. Trans. R. Soc. London, Ser. B **237**, 37 (1952).

[5] J. E. Rothenberg, Phys. Rev. A, 42, **682**, (1990).

[6] P. Kockaert, M. Haelterman, S. Pitois, and G. Millot, Appl. Phys. Lett. **75**, 2873 (1999).

[7] G. Millot, S. Pitois, P. Techfo Dinda, and M Haelterman, Opt. Lett., **22**, 1686, (1997).

[8] S. B. Cavalcanti, J. C. Cressoni, H. R. da Cruz, and A. S. Gouveira-Neto, Phys. Rev. A **43**, 6162 (1991).

[9] S. Pitois and G. Millot, Opt. Comm. **226**, 415 (2003).

[10] J. D. Harvey, R. Leonhardt, S. Coen, G. Wong, J. C. Knight, W. J. Wadsworth, and P. St. Russell, Opt. Lett. **28**, 2225 (2003).

[11] S. Coen and M. Haelterman, Phys. Rev. Lett. **79**, 4139 (1997).

[12] L.A. Lugiato and R. Lefever, Phys. Rev. Lett. **58**, 2209 (1987).

[13] K. Hansen, Opt. Express 11, 1503-1509 (2003).

[14] G. Kozyreff, S.J. Chapman, and M. Tlidi, Phys. Rev. E **68**, 015201(R) (2003).

[15] G. Kozyreff and M. Tlidi, Phys. Rev. E **69**, 066202 (2004).